

Turbulence quantification and sediment resuspension in an oscillating grid chamber

J.J. Orlins, J.S. Gulliver

662

Abstract An oscillating grid chamber has been developed to study sediment suspension, desorption of compounds from the resuspended sediment, and air–water mass transfer. The chamber is designed to allow researchers to study desorption of contaminants from cohesive sediments and the flux of those contaminants to the vapor phase. The chamber uses a single vertically oscillating grid driven by a DC motor and closed-loop controller. Sediment to be studied is placed in the bottom of the chamber and entrained into the water column by the turbulence generated by the oscillating grid. A two-component laser Doppler velocimeter (LDV) was used to measure the turbulent velocity field inside the chamber. Detailed mapping of the turbulent kinetic energy (TKE) produced by this grid arrangement was compared with established grid-stirred systems. At distances closer to the grid than two grid bar spacings, large lateral gradients exist in the TKE. The suspension of cohesive sediments was also studied using this chamber. Steady-state suspended sediment concentrations were achieved within 30 min for a variety of turbulence levels. By adjusting the grid operating parameters, the TKE can be set to simulate the turbulence found either at the bed or free surface in open-channel flow systems. With some care, the oscillating grid chamber can be used as a simple laboratory analogue to study various environmental processes within the flow or at either the sediment–water or air–water interface.

List of symbols

C_1, C_2, C_2	constants
f	grid oscillation frequency (T^{-1})
g	gravitational constant (LT^{-2})
h	depth of open-channel flow (L)
M	spacing between bars in oscillating grid (L)
S	grid stroke length (L)
S_{EGL}	slope of energy grade line in open-channel flow (m/m)
TKE	total kinetic energy of turbulence (L^2T^{-2})
TSS	total suspended solids concentration (ML^{-3})
U_*	bed shear velocity (LT^{-1})
U, V	instantaneous horizontal velocities (LT^{-1})
W	instantaneous vertical velocities (LT^{-1})
$\bar{U}, \bar{V}, \bar{W}$	mean velocities (LT^{-1})
u', v', w'	instantaneous velocity fluctuations (LT^{-1})
u', v', w'	root mean square (rms) turbulent velocity fluctuations (LT^{-1})
\overline{uw}	Reynolds stress (L^2T^{-2})
y	vertical distance from bed in open-channel flow (L)
z	vertical distance from grid (L)
α	constant
κ	Von Karman constant
ν	kinematic viscosity (L^2T^{-1})
Π	Cole's wake parameter
R_*	Reynolds number based on shear velocity and flow depth, U_*h/ν

1 Introduction

Contaminated sediments can pose a hazard to benthic and aquatic organisms. When such sediments are disturbed by either natural causes (such as storms or floods in rivers) or anthropogenic ones (such as dredging operations), the potential exists for contaminants to desorb from the sediments. Once the compounds are in the dissolved phase, they can be advected away from their original locale, and can also volatilize to the atmosphere. Understanding the desorption process and the means by which these compounds volatilize is of great importance in predicting their fate and transport.

Until recently, there has been little experimental work done on evaluating the release of contaminants from sediments and their flux to the vapor phase. Some researchers (Valsaraj et al. 1995) have proposed models describing the flux of semi-volatile organic compounds from sediments to water and atmosphere, but measurements of mass transfer rates have been lacking.

Received: 3 March 2001 / Accepted: 27 December 2002
Published online: 9 May 2003
© Springer-Verlag 2003

J.J. Orlins (✉)
Department of Civil and Environmental Engineering,
Rowan University, 201 Mullica Hill Road,
Glassboro, NJ 08028, USA
E-mail: orlins@rowan.edu
Tel.: +1-856-2565328
Fax: +1-856-2565242

J.S. Gulliver
St. Anthony Falls Laboratory, Department of Civil Engineering,
University of Minnesota, Mississippi River at 3rd Avenue SE,
Minneapolis, MN 55414, USA

This research was funded in part by support from the EPA's Hazardous Substance Research Center, South and Southwest, at Louisiana State University. The authors would like to thank K.T. Valsaraj and L.J. Thibodeaux for their support and collaboration in this research

To help remedy this situation, laboratory equipment has been developed to resuspend contaminated sediments under controlled conditions and measure the flux of contaminants to the water and vapor phases. The desired characteristics were that the device should be small enough to run simultaneous experiments on hazardous chemicals, should not have significant scale effects, and should simulate the turbulence of a free-surface flow. This laboratory-scale apparatus could then be used to quantify mass transfer from contaminated sediments to the water and vapor phases, and thus verify predictive models for use in real-world applications.

The equipment developed includes a number of square sediment resuspension chambers. Contaminated sediment is placed in the bottom of each chamber, and then entrained into the water column by turbulence generated by an oscillating grid. The flux of chemicals from the sediments to the water and air phases is then measured.

This paper describes the design of the chambers, quantification of the turbulence in the chambers, and tests of sediment resuspension under a variety of operating conditions. The relationship between turbulence at the free surface generated by the oscillating grid and air–water gas transfer will be examined in a forthcoming article. The use of these chambers for chemical flux measurements is described in Valsaraj et al. (1997).

2 Background

In natural systems, sediment resuspension is driven by turbulent shear stresses at the sediment–water interface. One way to simulate this process is with an oscillating-grid turbulence generator. Oscillating grids have been used since the 1950s to develop nearly isotropic, laterally homogeneous turbulence on a small scale, without the mean shear associated with water flowing over a surface. Numerous investigators have used these grids to study topics such as mixing across density interfaces (e.g., Thompson and Turner 1975; Hopfinger and Toly 1976), turbulence near an air–water interface (e.g., Brumley and Jirka 1987); sediment resuspension (e.g., Tsai and Lick 1986; Huppert et al. 1995); and desorption of contaminants from sediments (e.g., Connolly et al. 1983; Valsaraj et al. 1997). In this paper the turbulent kinetic energy will be mapped across a greater portion of the chamber, and the resuspension of cohesive sediments will be quantified. Both of these are important parameters for sediment–water chemical flux characterization.

2.1 Previous research

Initially, researchers used turbulence generated by oscillating grids as a one-dimensional analogue for studying mixing across stratified density interfaces. Such density interfaces are common in the natural environment, occurring as thermoclines and pycnoclines in reservoirs, lakes, and oceans. Functional relationships between the turbulence generated and the operational parameters of oscillating grids were developed by Thompson and Turner (1975) and Hopfinger and Toly (1976), among others.

These studies were aimed primarily at determining fluid entrainment rates across the interfaces. These researchers used square mixing tanks and single-plane grids made of square bars; turbulent velocities were measured with hot-film anemometers.

Mass transfer across a shear-free water–air interface has also been studied using grid-stirred tanks. Brumley and Jirka (1987) and Chu and Jirka (1992) examined the structure of turbulence close to the free surface, and related this to gas transfer by measuring dissolved oxygen profiles in the concentration boundary layer. The aim of these studies was to determine how the turbulence below the free surface affects mass transfer rates. These studies also used a square tank geometry and hot-film probes, and measured dissolved oxygen concentrations near the free surface with an oxygen microprobe.

Oscillating grids have been used to study resuspension of sediments. Tsai and Lick (1986) used a small, portable device to estimate the resuspension potential (i.e., the critical shear stress) for cohesive sediments in the field. Their device was a small (12.7 cm diameter) cylinder using a vertically oscillating perforated plate (instead of a grid of square bars) for the turbulence generator. They found that the mass of material eroded from the sediment–water interface was proportional to the oscillation frequency of the plate, but did not correlate this to the actual turbulence in their device. Rather, they related operational parameters to bed shear by means of an indirect calibration: they compared suspended sediment concentrations from their field device with those obtained in an annular flume. The bed shear in the flume was calculated based on velocity profile measurements; the assumption was made that the shear in their oscillating grid device must be equal to that in the flume for identical suspended sediment concentrations.

Huppert et al. (1995) also used an oscillating grid to study entrainment of non-cohesive sediments. For these studies, they used very dense solutions of silt-sized silicon carbide particles, and measured the entrainment of sediment to the overlying (sediment-free) water column. They compared these results with those obtained from experiments with non-particulate density interfaces; the fundamental difference is that the sediment particles responsible for the density gradient can settle out of solution. Since they utilized the same oscillating grid and tank as Thompson and Turner, the turbulence parameters derived from earlier studies were directly applicable. However, their results are not directly comparable with those of Tsai and Lick, because Huppert et al. did not use natural sediments, had a different tank geometry, and placed their oscillating grid at the bottom of their tank, in the dense suspension layer.

Brunk et al. (1996) used an array of horizontally oscillating grids to simulate open-channel flow turbulence as a function of depth. These researchers used their “differential turbulence column” to suspend sediment using both vertically homogeneous and vertically decaying turbulence fields. With a vertically decaying turbulence profile set up to model that found in open-channel flow, they found that the total suspended sediment concentration profiles followed conventional theories, and

concluded that their apparatus can be used to study many environmental processes. However, in the oscillating grid arrangement used in their work, there is a lateral variation in turbulence, which results in non-uniform turbulence conditions across the sediment–water interface.

Finally, Connolly et al. (1983) used an oscillating grid reactor to study the desorption of Kepone (a hydrophobic, organic compound) from natural sediments. For their experiments, they used a tall circular tank with a number of stacked oscillating grids, but they made use of Hopfinger and Toly's relationships between grid operational parameters and turbulence (which were developed for a square tank with a single grid). They found that equilibrium partitioning between the dissolved and sorbed phases of chemical is a linear function of dissolved phased concentration and an inversely non-linear function of suspended sediment concentration. In addition, they found that the partition coefficient is not only highly dependent on the chemical of concern, but also on the sediment type, indicating the complexity of sediment sorption equilibria.

The overall aim of the current project was to develop a device for resuspending cohesive sediments in a controlled manner that would allow measurement of the flux of chemical compounds from the sediments to the water and vapor phases. The well-established body of literature briefly described above provided the basis for selecting an oscillating grid mechanism to generate shear-free turbulence to resuspend the sediments. However, no previous work has been done on linking all of the aspects mentioned above (sediment resuspension ↔ turbulence ↔ air–water mass transfer) together in one experimental setup. In addition, detailed measurements of the turbulence within the mixing chamber were needed to characterize the relationship between turbulence, sediment entrainment, and mass transfer. Finally, it was desired to develop similitude relationships between turbulence generated by an oscillating grid and turbulence in a boundary layer flow.

2.2

Theory of turbulence in grid-stirred reactors

In a typical arrangement, a grid of square bars or mesh is oscillated vertically in a tank by an electric motor with an eccentric drive. The stroke (distance the grid travels up and down) and frequency of oscillation can be varied. The rms turbulent velocity fluctuations decay with the distance away from the grid. For a grid with square bars, it has been shown (Hopfinger and Toly 1976; DeSilva and Fernando 1992) that the horizontal (u' , v') and vertical (w') rms fluctuations can be described by

$$\begin{aligned} u' = v' &= \sqrt{\overline{u'^2}} = C_1 M^{0.5} S^{1.5} f z^{-1} \\ w' &= \sqrt{\overline{w'^2}} = C_2 M^{0.5} S^{1.5} f z^{-1} \end{aligned} \quad (1)$$

where S is the stroke length, f is the oscillation frequency, z is the distance away from a virtual origin, M is the mesh spacing of the grid, and C_1 and C_2 are constants that may depend on the geometric parameters of the grid. Here, u and w are the instantaneous velocity fluctuations ($u=U-U$; $w=W-W$), where U and W are the instantaneous

velocities and the overbars denote the mean values). Hopfinger and Toly report values of C_1 and C_2 of approximately 0.25 and 0.27, while DeSilva and Fernando (1992) measured values of approximately 0.22 and 0.26, respectively.

The empirical relationships for the turbulent velocity fluctuations do not hold until one reaches a significant distance from the grid. The turbulence near the grid is not homogeneous. Various relationships have been proposed for the limiting distance beyond which Eq. (1) are applicable. Atkinson et al. (1987) concluded that the relationships held for $z > 2M$, while DeSilva and Fernando (1992) found that for "small" strokes, the relationships held for $z > 4S$.

One of the advantages for using oscillating grids for studying turbulence and mixing phenomena is that there is no mean shear. Unlike a boundary-layer flow, where unidirectional shear is generated at the fixed boundaries, the oscillating grid produces no net flow direction, and thus no mean shear. This is not to say that there is no shear present at all; rather, the average shear over space and time is zero. The convenience of using a mean shear stress to characterize the turbulence is not possible in an oscillating grid chamber.

Since there is no mean shear in the oscillating grid chamber, the TKE of the turbulence can provide a basis for comparing sediment resuspension and mass transfer under differing operating conditions. The TKE can be defined from the rms velocity fluctuations:

$$\text{TKE} = \frac{1}{2}(u'^2 + v'^2 + w'^2) \quad (2)$$

Substituting in our physical parameters S , f , z , and M , and making the assumption that $v'=u'$, the TKE can be estimated as

$$\text{TKE} = \frac{1}{2}(2C_1^2 + C_2^2)(M^{0.5}S^{1.5}fz^{-1})^2 = \alpha(MS^3f^2z^{-2}) \quad (3)$$

where α would be 0.082 using DeSilva and Fernando's values of C_1 and C_2 .

3

Experimental aspects

3.1

Experimental setup

The design of the sediment resuspension/chemical flux chambers was derived from other oscillating grid arrangements reported in the literature. A square chamber was chosen for construction and LDV access considerations. A large plan-form area was desired to reduce the importance of wall effects in sediment entrainment and measurement of chemical fluxes across the air–water interface.

The sediment resuspension chamber was manufactured out of clear acrylic plastic, as shown in Fig. 1. The chamber is a cube 0.5 m on each side, with a tight fitting lid. The grid consists of an 8×8 mesh made out of 1.27 cm square aluminum bars, with a center-to-center spacing of 6.25 cm, and a bar length of 49 cm. The grid is connected to a 1/3 HP variable-speed DC motor by a stainless steel shaft and eccentric drive. A steel frame supports the drive motor and is permanently fastened to the lid.

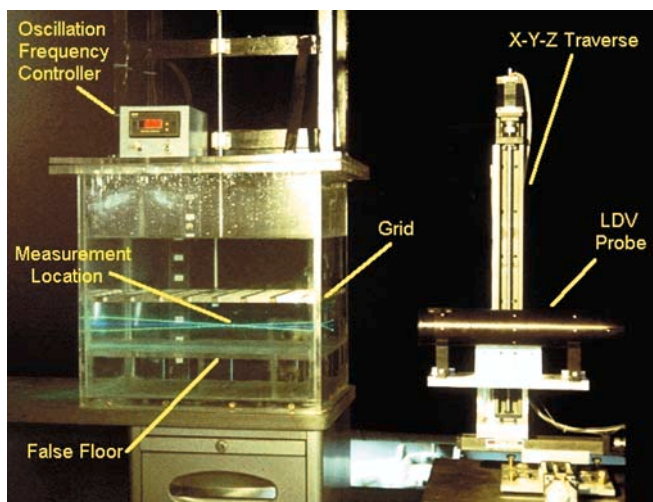


Fig. 1. Experimental setup

Two different methods were used to fasten the grid to the central drive shaft. In the initial grid configuration, a stainless steel plate was clamped across the central opening in the grid, and the drive shaft fastened through a hole in this plate. This design was chosen initially due to its relatively simple construction. In the second configuration tested, four smaller connecting shafts were fastened to the grid at the bar intersections closest to the grid center, and then drawn together to connect to the central shaft. This configuration resulted in a somewhat more cumbersome and fragile attachment, but the turbulence characteristics of the chamber were more uniform in the horizontal plane.

An acrylic guide is fastened to the back wall of the tank and prevents the grid from rotating in the tank. The grid stroke length can be adjusted from 2 to 12 cm by changing the attachment location of a connecting rod between the vertical shaft and eccentric drive. The oscillation frequency is set and maintained by a closed-loop programmable controller. Frequencies from 60 to 600 rev/min (1 to 10 Hz) can be maintained, depending on the stroke length.

Sediment is placed in the bottom of the chamber by removing the grid/lid/frame assembly. Water samples can be removed from the tank via a sampling port in the lid of

the tank and a siphon tube immersed in the water above the grid or via sampling ports at various elevations on the side of the tank.

3.2 Turbulence measurements

The turbulent velocity field inside the mixing chamber was measured using a two-component LDV, manufactured by TSI (St. Paul, Minn.). The system used a 5 W argon-ion laser, Colorburst beam splitter, 350 mm focal distance fiber-optic probe, Color Link receiving optics, and an IFA 755 signal processor. The system was controlled by a personal computer using TSI's FIND for Windows data acquisition and processing software.

For the velocity measurements, a false floor was installed at an elevation of 10.2 cm to simulate the sediment-water interface for three of the tests. The side walls of the tank were cleaned and polished using a cleaning compound made for acrylic plastic. Clean tap water was used for the tests; generally, there was enough natural particulate matter in the water that seeding was not required. For some tests, seed particles were added, but had little effect on data acquisition rates.

The fiber optic probe was mounted on a 3-axis traverse that was controlled by the pc-based data acquisition system. The probe was positioned to look through one of the side walls of the chamber and measure the vertical and one horizontal velocity component, also shown in Fig. 1. The probe could be positioned using the traverse for measurements at any location on one half of the chamber.

The LDV system was configured to measure velocities in the coincidence mode. This allowed direct computation of the Reynolds stress $\overline{u'w'}$. Data were collected at a measurement location for 100 s or until 10,000 measurements had been made. A frequency shift of 20 kHz was used for both the horizontal and vertical measurement channels. With the laser set to provide between 1 and 2 W output power, data collection rates were typically between 50 and 100 Hz.

In the initial series of tests with the original grid-mounting configuration, data were collected for three frequencies (3.0, 5.0, and 7.0 Hz) and a 3 cm stroke length and a total water depth of approximately 25 cm. Two

Table 1. Summary of turbulence measurement test conditions in oscillating grid tank

Test No.	Grid mounting ^a	Frequency (Hz)	Stroke (cm)	Water surface elevation (cm)	Bed elevation (cm)	Grid centerline elevation (cm)	Net water depth (cm)	Fig. No.
Detailed profile measurements								
3301	plate	3.0	3.0	35.0	10.2	23.2	24.8	3
3501	plate	5.0	3.0	35.0	10.2	23.2	24.8	4
3701	plate	7.0	3.0	35.0	10.2	23.2	24.8	5
3503	plate	5.0	3.0	35.0	0.0	23.2	35.0	6
3505	open	5.0	3.0	35.0	0.0	10.1	35.0	7
Detailed plane measurements								
3302	plate	3.0	3.0	35.0	10.2	23.2	24.8	8
3502	plate	5.0	3.0	35.0	10.2	23.2	24.8	9
3702	plate	7.0	3.0	35.0	10.2	23.2	24.8	10
3504	plate	5.0	3.0	35.0	0.0	23.2	35.0	11
3505	open	5.0	3.0	35.0	0.0	10.1	35.0	12

^a“Plate” indicates the original grid mounting method; “open” indicates the revised method

additional tests were run with the original and revised grid mounting, and a total water depth of 35 cm. The test operating conditions are summarized in Table 1.

For each condition, measurements were first made along four profiles at roughly 1 cm vertical increments. The profiles were intended to characterize the decay of turbulent velocity fluctuations and energy as a function of distance from the grid. In addition, data were collected along a number of planes above and below the grid. These measurements were intended to characterize the lateral variability of the turbulence parameters.

Measurement parameters included the horizontal and vertical average velocities U , W , the rms velocity fluctuations u' and w' , the relative turbulence intensities (e.g., u'/U), the Reynolds stress \overline{uw} , and the $u-w$ cross correlation coefficient. Raw data were stored in binary form for each measurement location. Summary files containing all of the parameters for each measurement location were created for each test in an ASCII (text) format using the FIND software. These data files were then used as input for further post-processing operations such as coordinate transformations, datum adjustments, and calculation of the TKE of the turbulence. These secondary processing operations were conducted using custom programs written in the Microsoft QuickBasic programming language.

3.2.1

Vertical profiles

Measurements of the turbulent velocities were made along four vertical profiles. Data were collected in both the region from the bottom of the tank to the grid and from the grid to the free surface. The first profile was located at the quarter point of the tank, at the center of an opening in the grid; the second profile was located at the intersection of two grid bars. The third and fourth profiles were located at symmetric positions on the other half of the tank. The profile locations are shown in Fig. 2a.

Data were collected at 1 cm intervals along the vertical profiles. Because of the configuration of the LDV optics, the measurement volume was not placed within approximately 1 cm of the bed or free surface. Likewise, measurements were not made within 1 cm of the bottom and top planes of the grid's motion.

3.2.2

Horizontal planes

In addition to the profile measurements, turbulent velocities were also measured along a number of horizontal planes above and below the grid. Measurements were taken at horizontal increments of one-half the grid spacing (3.125 cm), as shown in Fig. 2b. With this arrangement, data were collected coincident with the intersection of two grid bars, at the center of the openings in the grid, and at the midpoints of each bar segment. This resulted in a 15×8 grid of measurement points located in one half of the tank, for a total of 120 measurements per plane.

The measurement planes were located both above and below the grid. Above the grid, data were collected on planes near the free surface, midway from the free surface to the grid, and just above the grid. A similar arrangement was used below the grid (near grid, midway to bed, near bed).

3.3

Sediment entrainment measurements

A series of tests was conducted to determine the relationship between cohesive sediment resuspension and turbulence generated by the oscillating grid. The sediments tested came from University Lake, in Baton Rouge, Louisiana. The sediment composition was 10% sand, 76% silt, and 14% clay, with a organic carbon fraction of 0.041 and particle bulk density of 2.5 g/cm^3 .

The total mass of suspended solids was measured as a function of oscillation frequency, stroke length, and consolidation time. Eight tests were run, with frequencies of 150–650 rpm (2.5–10.8 Hz), strokes of 2, 3, and 4 cm, and consolidation times of 2 and 11 days.

Prior to each test, the sediments were removed from the chamber, completely mixed with a rotary mixer, poured back into the chamber, and allowed to consolidate for a standard period of time (2 or 11 days). After the consolidation period, the tank was slowly filled with water in a manner that did not disturb any of the sediments. The initial elevation of the sediments in the tank was typically 10–11 cm, and the water level 35 cm. The grid was adjusted to the desired stroke length (2, 3, or 4 cm), and positioned so that the center of motion was at an approximate elevation of 23 cm (i.e., 12–13 cm above the bed).

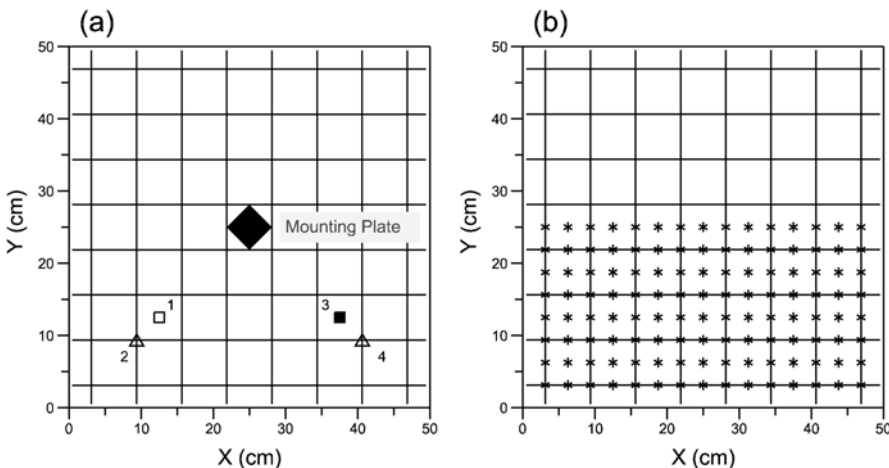


Fig. 2a, b. Velocity measurement locations

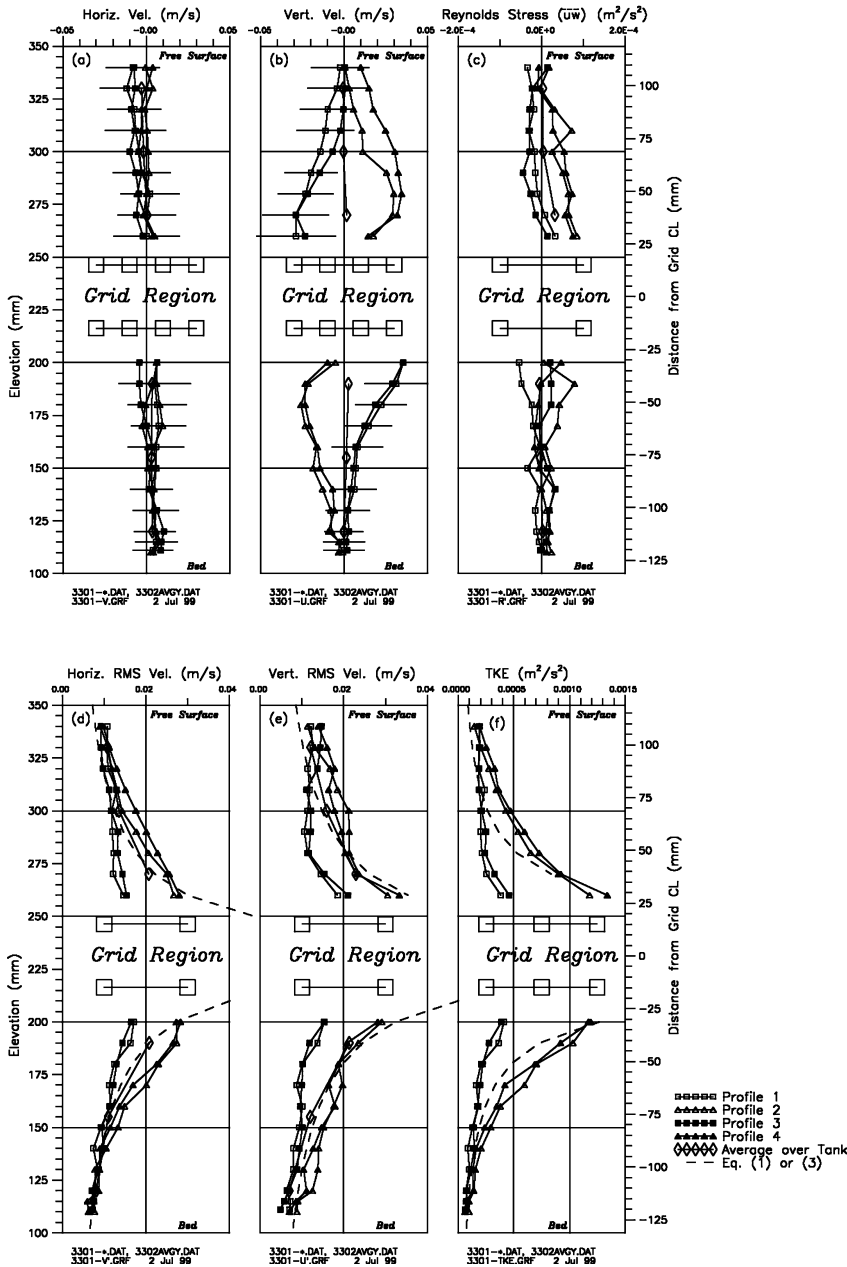


Fig. 3a-f. Velocity profiles, 3.0 Hz, original grid mounting, with false floor

For each test, the grid was oscillated at the lowest desired frequency, and water samples were withdrawn at regular intervals for later analysis. When an apparent steady-state suspended sediment concentration had been achieved, the oscillation frequency was increased, and maintained at the new level until a new steady-state concentration was reached. This procedure was repeated for a number of frequencies. Water analyses for the first few tests indicated that steady-state concentrations (within measurement uncertainty) were approached within 10–30 min. For later tests, the oscillation frequencies were then maintained for at least 30 min before being increased.

Water samples were withdrawn from the region between the grid and the free surface using a siphon, and placed in glass or plastic sample bottles for later analysis. TSS concentrations were determined by

filtering, drying, and weighing a known volume of sample water according to Standard Method 2540D (APHA 1992).

4 Results and discussion

4.1 Spatial quantification of turbulence

The results from the profile tests at the three frequencies tested are presented in Figs. 3, 4, 5, 6, and 7. In addition to the four profiles of the turbulence parameters, the figures show the average velocity components and the standard deviation of each, based on the velocity measurements taken along lateral planes in the tank, described above. Since the results from the three tests are qualitatively similar, the majority of the

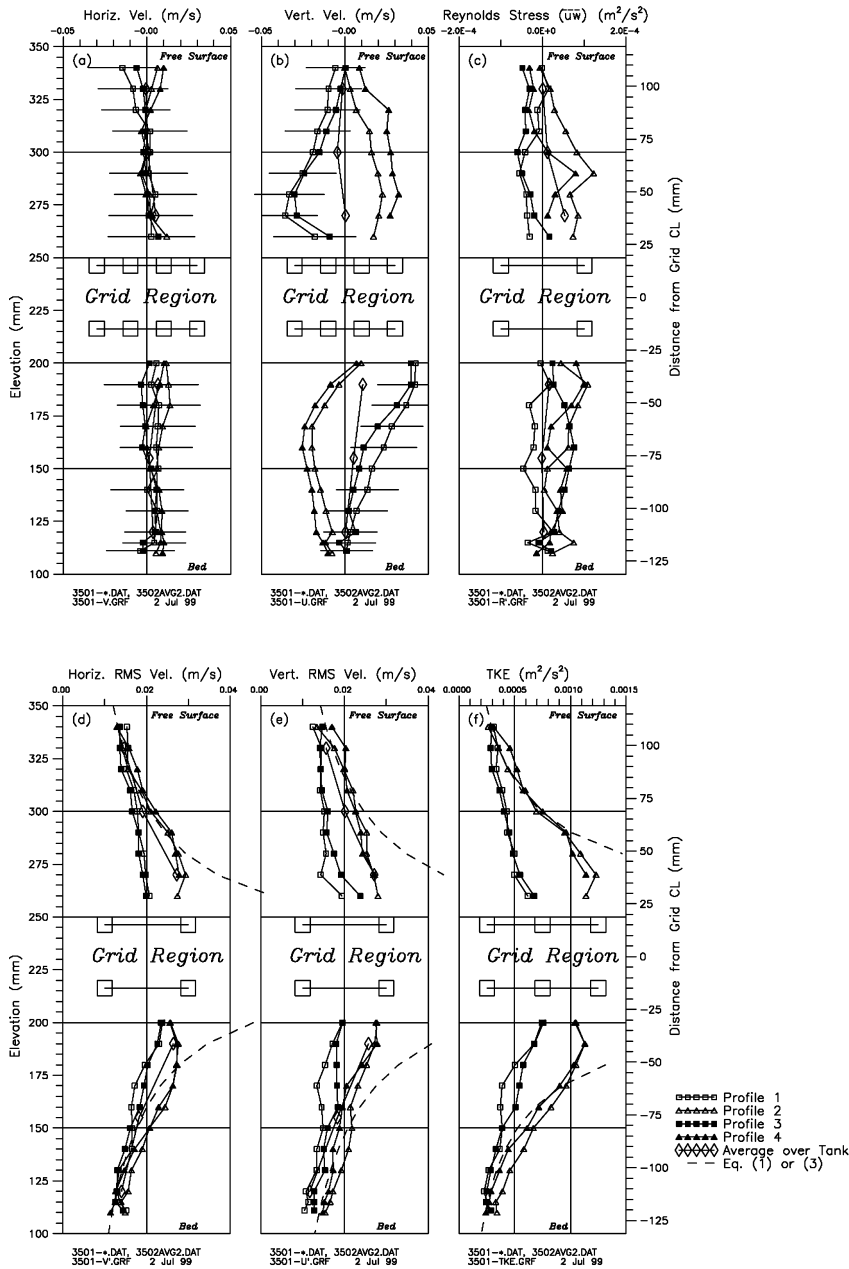


Fig. 4a-f. Velocity profiles, 5.0 Hz, original grid mounting, with false floor

comments will be restricted to the second case shown (Fig. 4), with the 3 cm stroke and oscillation frequency of 5.0 Hz.

4.1.1

Mean velocities

As can be seen from the profiles of the horizontal velocities (Fig. 4a) there appears to be little net lateral movement in the tank. Likewise, the mean vertical velocity (diamonds in Fig. 4b) is close to zero. (Here, the mean velocity is defined as the arithmetic average of the four profile measurements taken at a particular elevation.) However, the individual profiles in Fig. 4b indicate large-scale vertical mixing, which appears to be dependent on the location with respect to the grid. This is a direct result of the mounting plate holding the grid to the vertical drive shaft.

From the profiles, it appears that fluid is pushed away from the grid where the grid bars intersect (triangles, profiles 2 and 4), while it is pulled towards the grid at the open areas (squares, profiles 1 and 3).

The standard deviation of all horizontal and vertical velocity measurements at a particular elevation for profile 1 are shown as error bars in Fig. 4a and b, respectively.

4.1.2

Root mean square velocities

The rms of the turbulent velocity fluctuations are shown in Fig. 4d and e. In addition to the measured profiles and the averages over the whole tank, the expected rms velocity fluctuations based on the Hopfinger-Toly relationship (Eq. 1) are shown by the dashed line. It is apparent that the predictions are approached more closely by the data

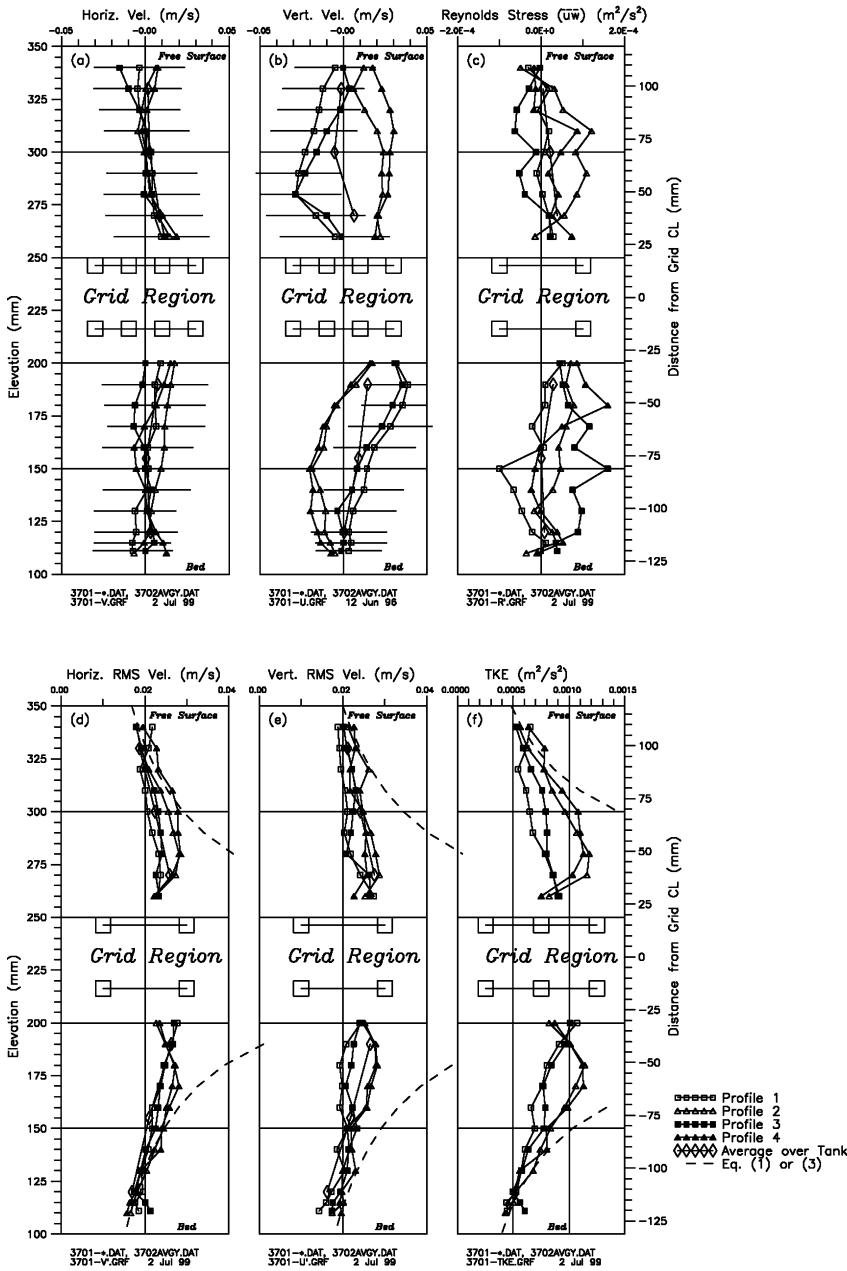


Fig. 5a-f. Velocity profiles, 7.0 Hz, original grid mounting, with false floor

away from the grid (i.e., near the bed and free surface). This is understandable, as the predictive relations are valid (based upon both Atkinson et al.'s and DeSilva and Fernando's criteria) for distances greater than 12.5 cm from the center of grid motion for these operating conditions; this is roughly the distance from the grid to the bed and water surface used in these experiments. For distances less than the criteria (which encompass the majority of the tank), the magnitude of the rms velocities above and below the openings in the grid (i.e., profiles 1 and 3) are considerably less than those coincident with the bar intersections (i.e., profiles 2 and 4).

4.1.3

Reynolds stress and total kinetic energy

The mean Reynolds stress, \overline{uw} , is quite small, as shown in Fig. 4c, with an average of zero and absolute value of

individual measurements less than roughly $2 \times 10^{-4} \text{ m}^2/\text{s}^2$. This makes sense, as this type of mixing chamber has no overall mean shear. It is interesting, however, to note that there is little variation of \overline{uw} with distance from the grid.

The total kinetic energy of the turbulence was calculated from the rms velocities using Eq. (2). Since the LDV system only measured velocities in one horizontal and the vertical directions (i.e., u and w), the other horizontal velocity (v) was estimated based on the symmetry of the tank. A similar estimate was made for the horizontal rms velocities.

The variation of TKE with depth is shown in Fig. 4f. Far from the grid, the measured values compare favorably with the TKE predicted using Eq. (3), which is based on the Hopfinger-Toly relationship for rms velocities. Again, magnitudes of the TKE are substantially less for profiles 1 and 3 than for profiles 2 and 4 close to the grid. In this

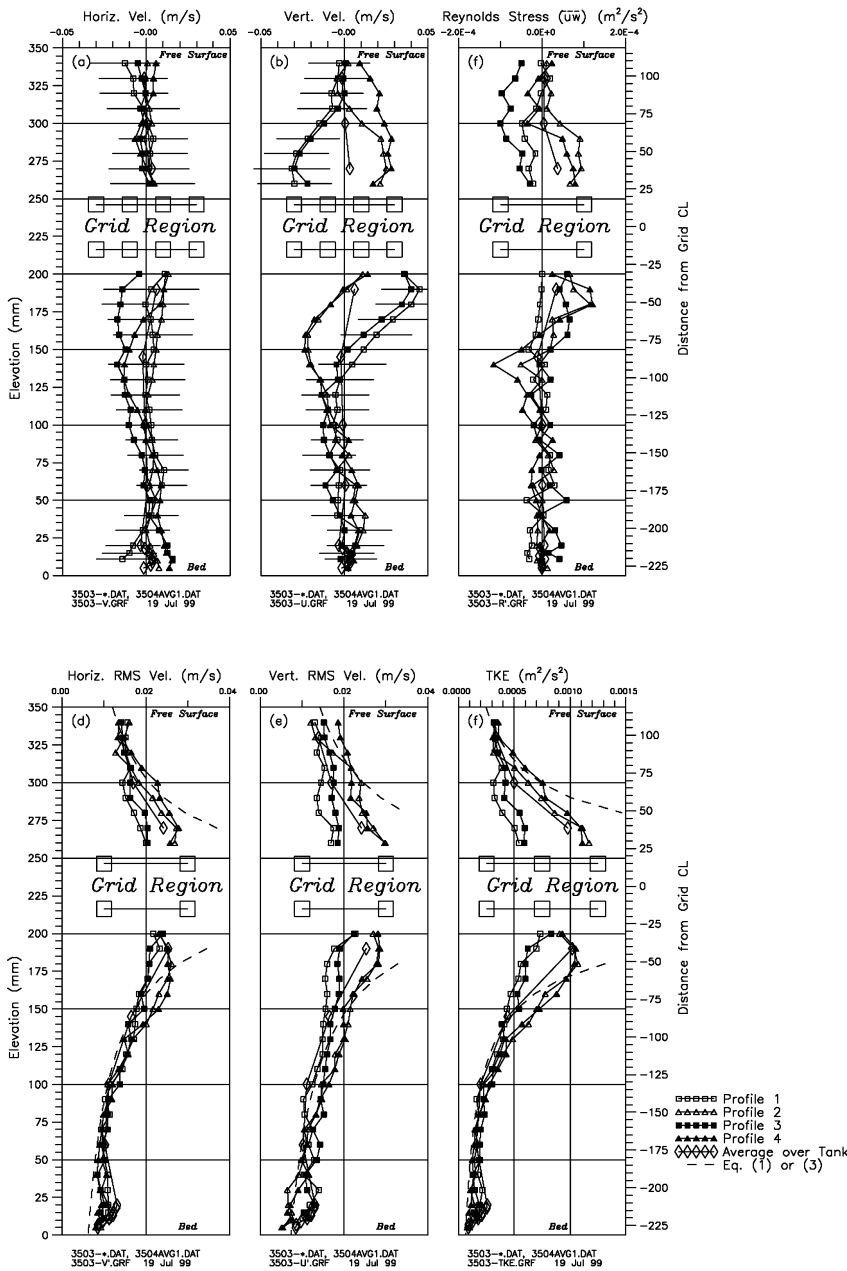


Fig. 6a-f. Velocity profiles, 5.0 Hz, original grid mounting, without false floor

region, it is likely that the TKE for profiles 1 and 3 is more greatly influenced by the wake from the oscillating grid. If this is true, the lesser of the two criteria, $z \geq 4S$ or $z \geq 2M$, for applying the Hopfinger-Toly relationship is probably most applicable.

Within the “near-grid” region, the TKE at locations coincident with grid bar intersections is approximately triple that at the “holes” between grid bars for an oscillation frequency of 3.0 Hz (Fig. 3), and approximately double for an oscillation frequency of 5.0 Hz (Fig. 4). This local horizontal variation in TKE decreases gradually with distance away from the grid, until the $z=2M$ or $z=4S$ criteria is reached. For the 7.0 Hz oscillation frequency test case (Fig. 5), this trend is reversed very close to the grid, with TKE values at the bar intersections slightly less than those above or below the “holes.” It appears that the local horizontal and vertical

rms velocity fluctuations are damped at the bar intersections for the higher oscillation frequencies, resulting in the relative reduction in TKE at these locations. However, the average of the TKE at all four profile locations does increase with increasing oscillation frequency, as expected.

The lateral variation in TKE is shown in Figs. 8, 9, 10, 11, and 12. Close to the grid, there are steep energy gradients, while farther from the grid (near the sediment-water and air-water interfaces) the turbulence is more uniform. This variation in TKE near the grid may also be seen in Fig. 4f, where the extremes in the variation are represented by the difference between the square and triangular symbols (i.e., profiles 1 and 3 versus profiles 2 and 4). In addition, with the original grid mounting configuration, there exists a region of elevated TKE near the center of the tank (Figs. 8, 9, 10, and 11).

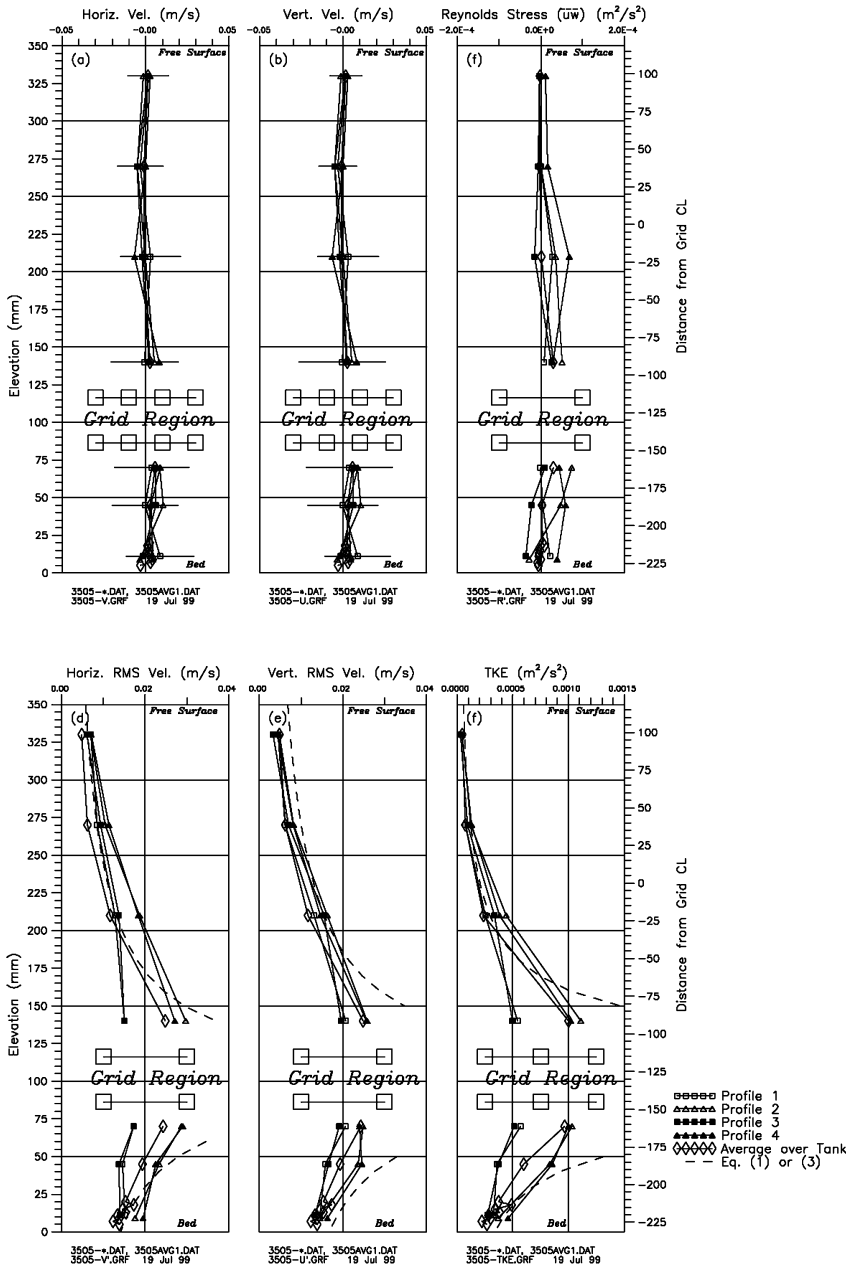


Fig. 7a-f. Velocity profiles, 5.0 Hz, revised grid mounting, without false floor

4.1.4 Effect of false floor

The initial turbulence measurement tests were conducted with a false floor in the bottom of the tank, to simulate the physical boundary condition of the sediment-water interface. One test was conducted without the false floor, such that the oscillating grid was able to mix fluid in the entire tank volume. Profiles from these tests are shown in Figs. 4 and 6, and perspective views of the TKE in planes above and below the grid are shown in Figs. 9 and 11.

Quantitatively, the results between the two different tests are similar. The net horizontal velocities throughout the depth of the tank are close to zero (Figs. 4a and 6a). Likewise, the net average vertical velocities (diamonds in Figs. 4b and 6b) are close to zero, but as with the other test cases, there are large local variations, depending on whether the measurement profile was located under a grid bar intersection or hole.

Without the false floor, it appears that there are small secondary currents at the bottom of the tank (Fig. 6a, elevation 0–25 mm). These result in a slight increase in the rms velocities near this fixed boundary, and a corresponding increase in TKE. Since the distance from the grid to the free surface was the same between these two tests, there appear to be no differences in the profiles above the grid.

The overall spatial distribution of TKE (Figs. 9 and 11) appear quite similar with and without the false floor. The apparent TKE (color) variations between the two cases result from slight variations in the location of the visualization plane above and below the grid.

4.1.5 Effect of grid mounting system

A region of elevated TKE exists near the center of the tank for each of the test cases with the original mounting plate.

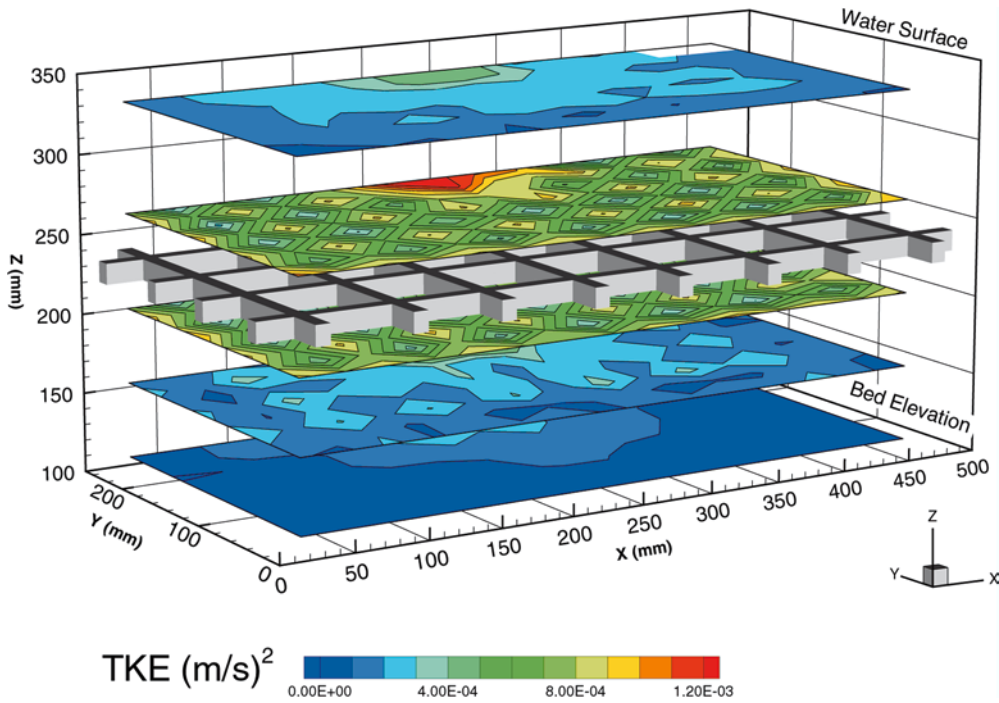


Fig. 8. Spatial distribution of TKE, 3.0 Hz, original grid mounting, with false floor

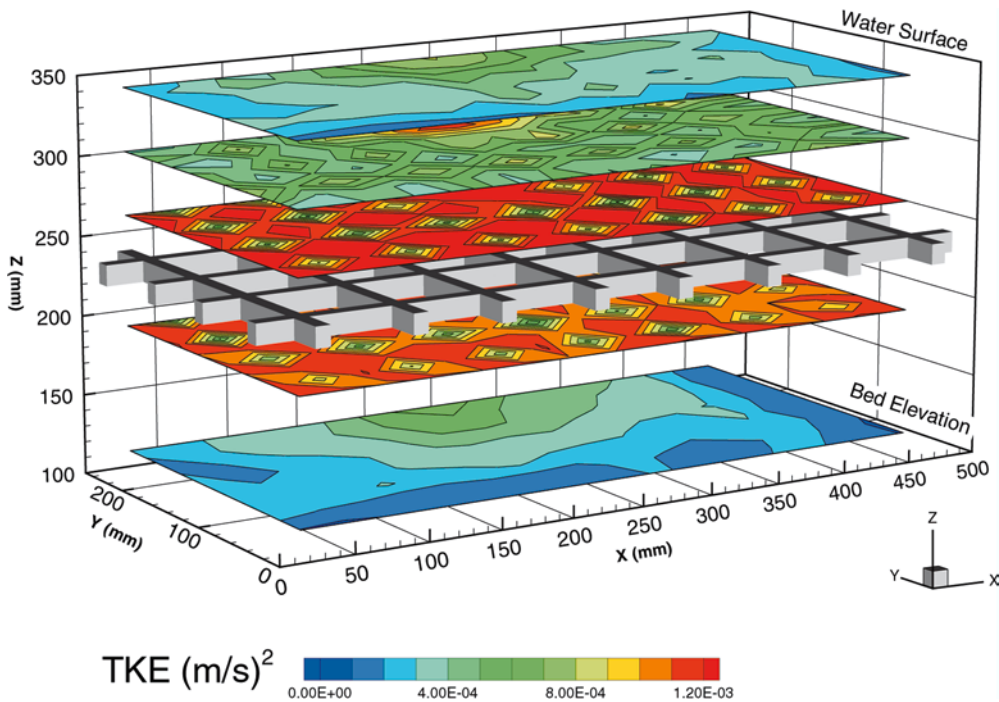


Fig. 9. Spatial distribution of TKE, 5.0 Hz, original grid mounting, with false floor

This can be seen as a “bulls-eye” in the TKE contours shown in Figs. 8, 9, 10, and 11 at the (x, y) location (250, 250). The support plate covered a large portion of the center-most grid open space, and set up localized secondary currents with high rms velocities, as can be seen in Figs. 3b, 4b, 5b, and 6b.

To reduce these secondary currents and the associated elevated turbulence levels, the rigid mounting plate was replaced with four small shafts, connected directly to the grid at the bar intersections closest to the center of the grid.

With this configuration, LDV measurements were only taken in the planar configuration, with three measurement elevations below the grid and four above. Measurements corresponding to the profile locations shown in Fig. 2a were extracted from this data set, and are shown plotted as profiles in Fig. 7. The spatial distribution of TKE for this configuration is shown in Fig. 12.

With the revised mounting configuration, both the horizontal and vertical velocities in each profile have lesser magnitudes than with the original

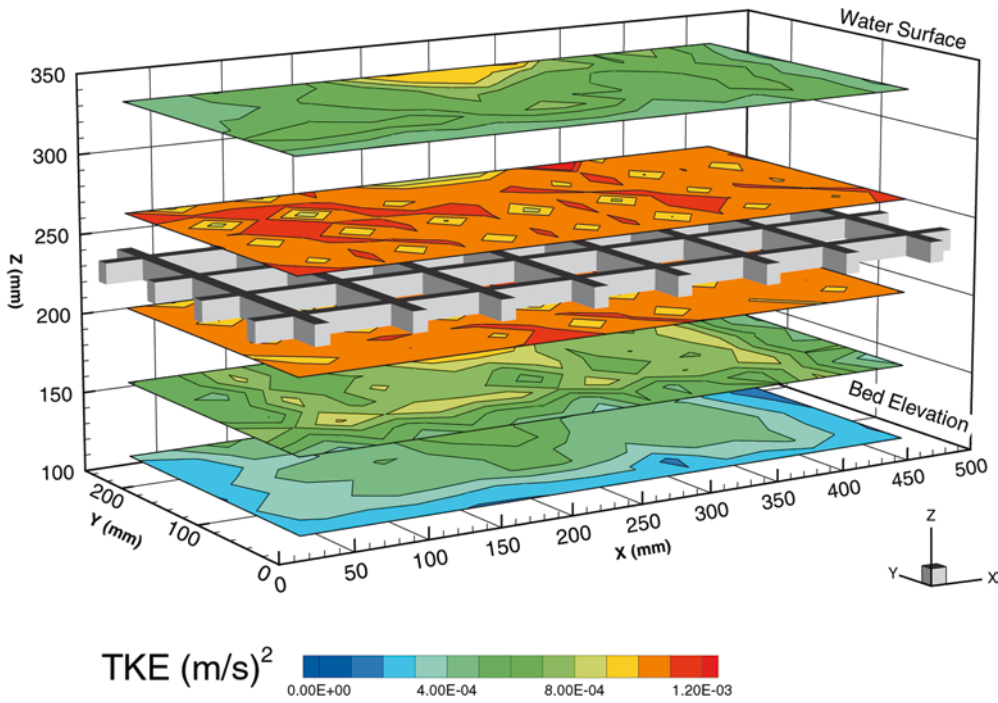


Fig. 10. Spatial distribution of TKE, 7.0 Hz, original grid mounting, with false floor

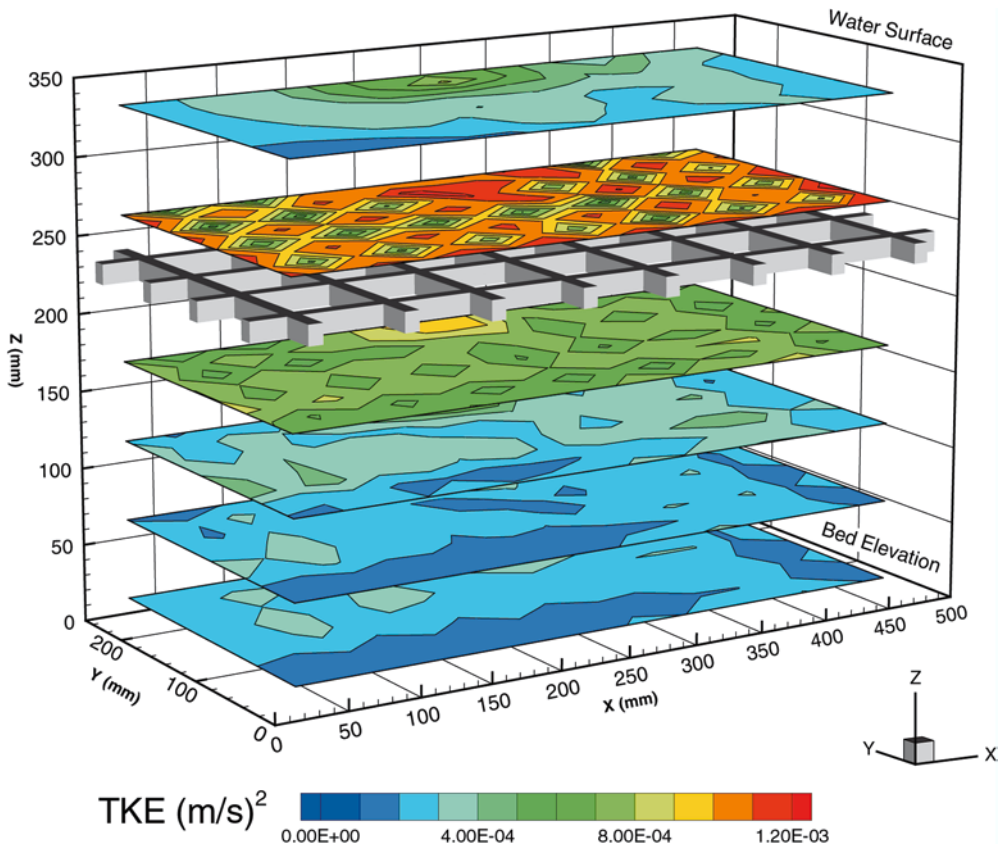


Fig. 11. Spatial distribution of TKE, 5.0 Hz, original grid mounting, without false floor

mounting, as can be seen by comparing Figs. 6 and 7. Especially notable are the vertical velocities close to the grid (Figs. 6b and 7b). With the revised mounting configuration, the “push-pull” effect of the mounting plate is eliminated, resulting in more uniform velocity profiles.

The overall spatial distribution of TKE is much more uniform at any given elevation with the revised mounting, as can be seen by comparing Figs. 9, 11, and 12. With the revised mounting, there is no “bullseye” region of higher TKE at the center of the tank. However, the smaller-scale gradients in TKE still exist in the region close to the grid,

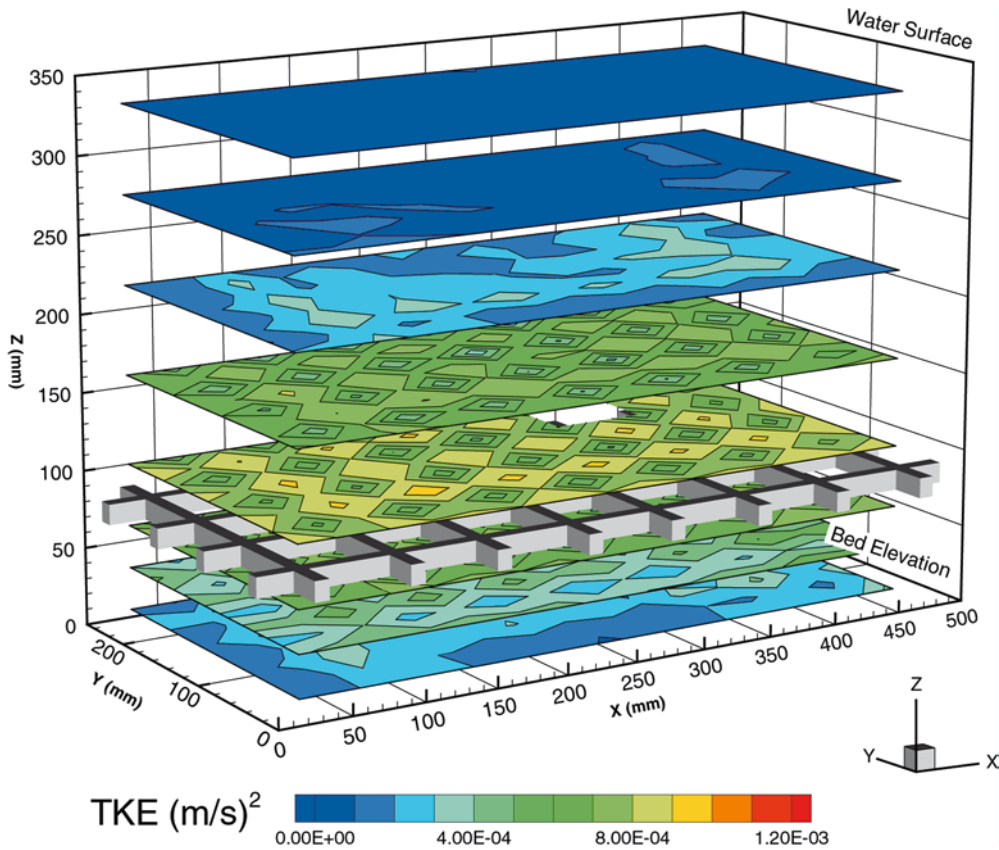


Fig. 12. Spatial distribution of TKE, 5.0 Hz, revised grid mounting, without false floor

with elevated values at the bar intersections and lower values at the grid openings.

4.2 Sediment entrainment

The time-history of suspended sediment concentration for a representative test is shown in Fig. 13. Initially, at low turbulence levels (i.e., low oscillation frequencies), there was no sediment entrainment. During this period of testing, the water samples withdrawn represent the nominally clean tap water introduced to the tank, and provide an indication of the lower limit of quantitative analysis that was obtained. As the energy input to the system was increased by raising the grid oscillation frequency, the instantaneous shear at the bed raised above the threshold critical shear. After this point, entrainment occurred rapidly. Steady state concentrations were achieved within 30 min, with a maximum observed TSS load of about 3.0 g/l at the highest oscillation frequency.

To allow interpretation of the TSS data, the total kinetic energy (TKE) at the sediment-water interface was estimated for each operating condition using Eq. (3). The steady-state suspended sediment concentrations were then plotted for each test as a function of the estimated TKE, as shown in Fig. 14.

There is a distinct difference in resuspension between the sediments allowed to consolidate for 11 days and those tested after only 2 days. This is expected, as cohesive sediments that have a greater consolidation will require a greater critical shear to initiate resuspension from the bed.

At a TKE of roughly $1.2 \times 10^{-3} \text{ m}^2/\text{s}^2$, however, the total suspended solids concentration was similar for both consolidation times.

4.3 Use of the chamber as an analogue to natural systems

Since an oscillating grid chamber produces reproducible levels of uniform turbulence, it can be used as a one-dimensional analogue to a boundary layer flow in natural systems.

The uni-directional orientation of a boundary layer flow allows turbulence to be readily quantified through a mean boundary shear. For the confined boundary layer of open channel flow, Nezu and Nakagawa (1993) note that the free-stream, transverse, and vertical rms velocity fluctuations (u' , v' , w') can be expressed as

$$\begin{aligned} u'/U_* &= 2.30 \exp(-y/h) \\ v'/U_* &= 1.27 \exp(-y/h) \\ w'/U_* &= 1.63 \exp(-y/h) \end{aligned} \quad (4)$$

where U_* is the bed shear velocity, y is the distance from the bed, and h is the flow depth. Of course, at $y=0$ all three fluctuating velocity components are equal to zero and at $y=h$ the vertical fluctuating velocity component w' generally approaches zero.

With an oscillating grid, however, the simplification of turbulence represented by a mean boundary shear does not work. Although there is shear produced by an oscillating grid, the temporal mean shear is zero, as shown in Figs. 3c, 4c, and 5c. We must therefore use more robust

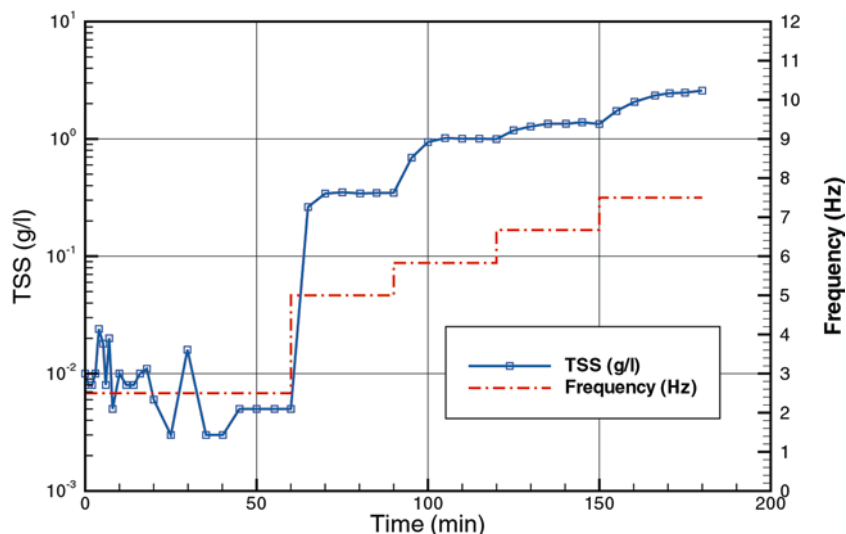


Fig. 13. Suspended sediment concentration vs. time

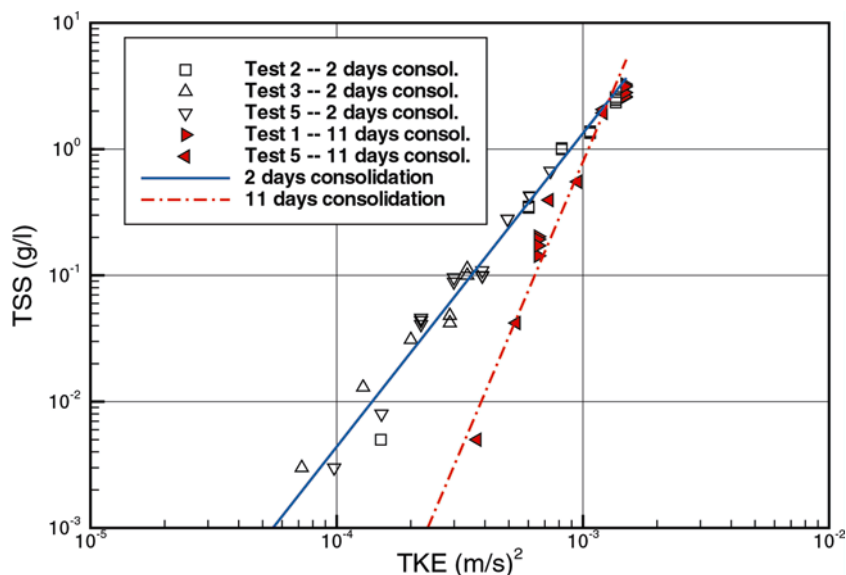


Fig. 14. Suspended sediment concentration vs. TKE

terms such as the total kinetic energy of the turbulence to quantify the turbulence.

4.3.1

Total kinetic energy

The rms expressions in Eq. (4) can be combined using Eq. (2) into the form:

$$\text{TKE}/U_*^2 = 4.78 \exp(-2y/h) \quad (5)$$

These expressions can allow estimation of the TKE near the bed and free surface in open channel flows.

Considering the case of normal flow in an open channel, the shear velocity is related to the flow depth and channel slope: $U_* = (ghS_{\text{EGL}})^{1/2}$, where S_{EGL} is the slope of the energy grade line and g is the gravitational constant. Thus,

$$\text{TKE} = 4.78 \exp(-2y/h)(ghS_{\text{EGL}}) \quad (6)$$

The limiting cases are at the fixed bed ($y/h \rightarrow 0$) and free surface ($y/h \rightarrow 1$). In these cases, the total

kinetic energy is simply a function of the depth of flow and slope:

$$\begin{aligned} \text{TKE}_{\text{bed}} &= 4.78(ghS_{\text{EGL}}) \\ \text{TKE}_{\text{FS}} &= 0.65(ghS_{\text{EGL}}) \end{aligned} \quad (7)$$

To simulate the turbulence levels close to the bed associated with a natural flow, the operational parameters of the oscillating grid (stroke, frequency, etc.) can be adjusted to achieve the desired level of turbulence. For the case of open-channel flow turbulence close to the bed, this can be done by substituting Eq. (3) into (7), and solving for either the stroke length, frequency, or distance from the grid to the bed:

$$\frac{S^3 f^2}{z^2} = \frac{4.78}{\alpha M} (ghS_{\text{EGL}}) \quad (8)$$

To simulate other conditions (e.g., estuarine environments), the same approach can be used, provided a suit-

able expression for the TKE present in that system can be found.

4.3.2

Reynolds stress

The Reynolds stress of an open-channel flow has been investigated in a manner similar to the rms velocity fluctuations shown in Eq. (4). Nezu and Nakagawa (1993) express the mean Reynolds stress as

$$-\overline{uw}/U_*^2 = (1 - y/h) - V_t$$
$$V_t(y/h) \equiv \frac{1}{\kappa R_*} \left[\left(\frac{h}{y} \right) + \pi \Pi \sin\left(\pi \frac{y}{h}\right) \right] \quad (9)$$

where κ is the Von Karman constant, Π is Cole's wake parameter, and R_* is the Reynolds number based on shear velocity and flow depth.

As mentioned previously, the convenience of using the mean shear stress to characterize turbulence in an oscillating grid chamber is not possible. This is borne out by the fact that the measurements of the Reynolds stress in the present study do not show any consistent trends with distance from the oscillating grid. The maximum absolute value of the individual profile measurements was less than $2 \times 10^{-4} \text{ m}^2/\text{s}^2$ for all test conditions investigated. For comparison, the mean Reynolds stress (calculated using Eq. 9) for an open channel flow such as the Mississippi River near Minneapolis ranges from about $6 \times 10^{-8} \text{ m}^2/\text{s}^2$ at the water surface to about $4 \times 10^{-3} \text{ m}^2/\text{s}^2$ at the river bed. Although the Reynolds stress is not an appropriate scaling parameter (versus the TKE of the turbulence), we can see that the oscillating grid thus produces Reynolds stress levels comparable with those nearer the bottom of a large open channel flow.

5

Conclusions

The primary objectives of the current work were to develop a laboratory-scale device for studying the release of chemical compounds from sediment entrained in the water column; characterize the relationship between turbulence and sediment entrainment in the device; and to develop similitude relationships between the turbulence in the device and that found in a boundary layer flow. The resulting equipment is a square plastic flux chamber with turbulence generated by a vertically oscillating grid. Measurements were made of turbulence generated by this device and sediment entrainment for a variety of operating conditions, and relationships were developed between turbulence in open-channel flows and the operational parameters of the oscillating grid. This device can be used to quantify mass transfer from contaminated sediments to the water and vapor phases, and thus be used to help verify predictive models of contaminant transport in real-world applications.

The turbulent flow field in the oscillating grid chamber described here is fairly uniform at sufficient distances away from the grid, regardless of the method used to attach the grid to the drive shaft. When a solid plate is used to attach the grid to the drive shaft, a region of higher turbulence exists in the center of the

tank, coincident with the plate. This "bull's-eye" area of elevated turbulence levels is not present when the grid is fastened to the drive shaft in a less obtrusive manner. In addition, the rms velocity fluctuations and total kinetic energy are described well by the Hopfinger-Toly relationship (Eqs. 1 and 3) at distances greater than about twice the grid bar spacing (i.e., 12.5 cm for the grid used in this work). However, at locations closer to the grid, there exist large gradients in the rms velocities and TKE.

This type of mixing chamber is capable of suspending cohesive sediments under a variety of conditions. Steady-state suspended sediment concentrations are reached fairly quickly (10–30 min). The maximum TSS concentrations achieved ranged from 0.01 to 3.0 g/l for the sediments tested. The amount of sediment entrained was a function of the energy input to the system from the oscillating grid and the sediment consolidation time.

The oscillating grid mixing chamber can be used as an analogue to open-channel flow systems by setting operational parameters of the grid (stroke, frequency, etc.) such that the total kinetic energy of the turbulence matches that expected either at the bed or free surface for an open channel flow. In this manner, the chamber can serve as a simple, self-contained test bed for evaluating the flux of chemical from sediments to water and from water to the atmosphere. Since the chamber can be sealed off from the laboratory atmosphere, chemical flux tests using hazardous or toxic compounds can be performed in relative safety. Due to the predictable and reproducible nature of the turbulence generated by the oscillating grid, replicate tests of sediment resuspension and chemical fluxes can be readily accomplished.

References

- APHA (1992) Standard methods for the examination of water and wastewater, 18th edn. American Public Health Association, American Water Works Association, and Water Environment Federation, Washington, DC
- Atkinson JF, Damiani L, Harleman DRF (1987) A comparison of velocity measurements using a laser anemometer and a hot-film probe, with applications to grid-stirring entrainment experiments. *Phys Fluids* 30:3290
- Brumley BH, Jirka GH (1987) Near-surface turbulence in a grid-stirred tank. *J Fluid Mech* 183:235–263
- Brunk B, Weber-Shirk M, Jensen A, Jirka G, Lion LW (1996) Modeling natural hydrodynamic systems with a differential-turbulence column. *J Hydr Eng* 122:373–380
- Chu CR, Jirka GH (1992) Turbulent gas flux measurements below the air-water interface of a grid-stirred tank. *Int J Heat Mass Transfer* 35:1957–1968
- Connolly JP, Armstrong NE, Miksad RW (1983) Adsorption of hydrophobic pollutants in estuaries. *J Environ Eng* 109:17–35
- DeSilva IPD, Fernando HJS (1992) Some aspects on mixing in a stratified turbulent patch. *J Fluid Mech* 240:601–625
- Hopfinger EJ, Toly JA (1976) Spatially decaying turbulence and its relation to mixing across density interfaces. *J Fluid Mech* 78:155–175
- Huppert HE, Turner JS, Hallworth MA (1995) Sedimentation and entrainment in dense layers of suspended particles stirred by an oscillating grid. *J Fluid Mech* 289:263–293
- Nezu I, Nakagawa H (1993) Turbulence in open-channel flows. A.A. Balkema, Rotterdam

- Thompson SM, Turner JS (1975) Mixing across an interface due to turbulence generated by an oscillating grid. *J Fluid Mech* 67:349–368
- Tsai CH, Lick W (1986) A portable device for measuring sediment resuspension. *J Great Lakes Res* 12:314–321
- Valsaraj KT, Ravikrishna R, Orlins JJ, Smith JS, Gulliver JS, Reible DD, Thibodeaux LJ (1997) Sediment-to-air mass transfer of semi-volatile contaminants due to sediment resuspension in water. *Adv Environ Res* 1:145–156
- Valsaraj KT, Thibodeaux LJ, Reible D (1995) Modeling air emissions from contaminated sediment dredged materials. In: Demars KR, Richardson GN, Yong RN, Chaney RC (eds) *Dredging, remediation, and containment of contaminated sediments*, ASTM STP 1293. American Society for Testing and Materials, Philadelphia, Penn., pp 227–238